Polym. Bull. (2015) 72:2089–2104
DOI 10.1007/s00289-015-1391-7

ORIGINAL PAPER

Synergistic effect of allophane with intumescent flame retardants on thermal behavior and fire retardancy of polypropylene

Xinqing Su[1] · Dongyan Li[1] · Jie Tao[1] · Qiwei Dai[1]

Received: 18 January 2015 / Revised: 18 March 2015 / Accepted: 15 April 2015 /
Published online: 22 April 2015

Abstract The effects of allophane (ALL) as a synergistic agent on the flame retardancy and thermal stability of intumescent flame-retardant (IFR) polypropylene composites were studied by limiting oxygen index (LOI), UL-94 test, cone calorimeter test (CONE) and thermogravimetric analysis. The incorporation of ALL led to enhanced thermal stability, LOI value and UL-94 ratings. CONE tests indicated that heat release rate, peak rate of heat release, smoke production rate, total smoke production and mass loss values of PP/IFR/ALL sample were much lower than those of PP/IFR and pure PP samples. Fourier transform infrared spectrometry result proved the presence of silicoaluminophosphate which can act as a catalytic agent to enhance the oxidative dehydration crosslinking charring process. Scanning electron microscopy and Raman spectra observation demonstrated that ALL could promote forming homogenous and compact char layer. The mechanical properties of PP composites were also improved by the loading of ALL.

Keywords Allophane · Polypropylene · Synergistic · Intumescent flame retardant

Introduction

Polypropylene (PP) is used worldwide in many fields due to its excellent mechanical properties, low density and good chemical resistance [1]. However, the applications of PP products are confined by its flammability and poor flame resistance [2]. Traditionally, halogen-containing flame retardants, alone or in conjunction with antimony trioxide, are the most effective flame retardants for PP. Nevertheless, the

✉ Xinqing Su
sxq_msc@nuaa.edu.cn

[1] College of Material Science and Technology, Nanjing University of Aeronautics and Astronautics, 29 Yudao Street, Nanjing 210016, People's Republic of China

use of these flame retardants has been restricted for safety and environmental concerns [3]. To satisfy the requirements of environmental friendly, some halogen flame retardants are replaced by some halogen-free flame retardants. Recent research indicates that intumescent flame retardants (IFR) with low toxicity and low smoke are so far the best flame retardants to replace halogen flame retardants [4, 5]. In general, intumescent flame retardant contains three active ingredients: carbon catalyst (or acid source), char-forming agent (or carbonization agent), blowing agent [6, 7]. The compounds used as carbon catalysts generally are inorganic acid or precursor of the acids. Char-forming agents are mostly hydroxyl-containing compounds. Blowing agents are the contents which can produce noninflammable gases on heating [8].

It was shown that the combination of ammonium polyphosphate (APP) and pentaerythritol (PER) is an effective intumescent flame retardant (IFR) in PP [9, 10]. However, this traditional IFR has some drawbacks, such as low flame-retardant efficiency, poor thermal stability and poor compatibility with polymer matrix. To improve the flame retardancy, synergistic agents have been used in IFR systems, such as silicate clay [11–13]. The main advantage of synergistic agents is that they can achieve significant enhancement of thermal stability and fire retardancy efficiency with a low loading. Many papers have shown that a low loading of silicate clay as synergistic agent such as zeolite and halloysite in polymer matrices demonstrates significant enhancement of thermal stability and fire retardancy for polymer composites [12–14].

Allophane (ALL), a natural clay distributed throughout the world, is a hydrated aluminosilicate ($1\text{-}2SiO_2{\cdot}Al_2O_3{\cdot}5\text{-}6H_2O$) with a 3.5- to 5.0-nm-sized hollow spherical structure [15, 16]. However, as a kind of silicate clay, there are no reports about ALL used in PP/IFR system.

In this paper, allophane (ALL) derived from hydrothermal synthesis as a novel synergistic agent was introduced into PP/IFR system. The synergistic effect of ALL combined with IFR on flame retardancy and thermal stability of PP was investigated by LOI, UL-94, CONE test and TGA. FT-IR was used to identify the composition of the residue char obtained from CONE test. SEM observation was employed to investigate the micromorphology of the char residue. The mechanical properties of PP composites were also studied.

Experimental

Materials

The matrix polymer used in this study was PP (1215-c, pellets products). Ammonium polyphosphate (APP) was supplied by Xingxing flame retardant Co., Ltd. Pentaerythritol (PER, white powder, AR grade) and aluminum chloride ($AlCl_3$, white powder, GR grade) were provided by Sinopharm Chemical Reagent Co., Ltd. Sodium silicate, ortho ($NaSiO_4$) was purchased from Adamas Reagent Co., Ltd. ALL was synthesized in our laboratory.

Synthesis of ALL

The precursor gels for the allophane synthesis were prepared by mixing and stirring (for 1 h) of 100 mM of $NaSiO_4$ and $AlCl_3$. The sodium chloride formed was removed by centrifugation at the speed of 5000 rpm for 5 min. The precursors were then autoclaved at 100 °C for 48 h. The resulting materials were washed with distilled water repeatedly until they reached neutral pH. Subsequently, the obtained samples were dried at 40 °C in an oven [17].

Preparation of PP blends

All flame-retarded PP composites were prepared using the CM-reciprocating single-screw extruder (CM-30). The temperature range of the single-screw extruder was set at 160–200 °C. Compositions are listed in Table 1. The resulting compounds were subsequently dried in an oven and were further injection molded into bars with an injection molding machine (HTF86X1) for fire and mechanical properties' characterizations. The composites were injected into standard testing bars for the tests of combustibility.

Measurements

XRD diffraction patterns were recorded using a Japan Rigaku in the reflection mode at room temperature.

Samples for FT-IR measurement were mixed with KBr powders and pressed into a tablet. The FT-IR spectra were obtained using an FT-IR spectrophotometer (NEXUS 670) in the range from 390 to 3700 cm^{-1}.

Thermogravimetric analysis was carried out with a NETZSCH STA409 PC thermoanalyzer instrument using about 10 mg samples. The samples were heated from room temperature to 700 °C in a 50 ml/min flow of N_2 at scanning rate of 10 °C/min.

Limiting oxygen index was carried in an HC-2 oxygen index meter (Jiangning Analysis Instrument Company, China) with samples' measurement $120 \times 10 \times 4$ mm^3, following the procedure described in the ASTM D2863 standard.

Table 1 Effect of ALL on the LOI and UL-94 of PP/IFR systems (IFR: APP/PER = 3/1)

Sample code	PP (%)	IFR (%)	ALL (%)	LOI (%)	UL-94 rating
PP	100	0	0	18	No rating
PP/IFR	75	25	0	27	V-1
PP/IFR/ALL1	74	25	1	29	V-1
PP/IFR/ALL2	73	25	2	35	V-0
PP/IFR/ALL3	72	25	3	34	V-1
PP/IFR/ALL4	71	25	4	31.5	V-1
PP/IFR/ALL5	70	25	5	30	V-1

UL-94 tests were performed on vertical testing apparatus (CZF-2, Jiangning Analysis Instrument Factory, China) with sample dimensions of 130 × 13 × 3 mm^3 according to the UL-94 test standard.

CONE tests were performed according to ISO5660 standard procedures. All samples (100 × 100 × 3 mm^3) were tested at horizontal position with the heat radiant flux density of 35 kW/m^2. The experimental error of data from the cone calorimeter was about 5 %.

Laser Raman spectroscopy measurements were carried out at room temperature with a JY HR800 laser Raman spectrometer (JY Co., French).

Scanning electron microscopy was used to examine the morphology of the residue char obtained from CONE test using a SUPRA 55/55VP SEM, whose accelerating voltage was 15 kV. The surface of residue char was sputter coated with gold layer before examination.

The tensile tests were conducted on a universal testing machine (Model CMT-5105) according to GB/T1039-1992. The testing speed for tensile strength was 50 mm/min. The izod notched impact strength was measured on a pendulum impact testing machine (Model XJ-300A) according to GB/T1043-93.

Results and discussion

Characterization of synthetic allophane (ALL)

Figure 1 shows the XRD pattern of synthetic ALL. The synthetic ALL exhibits broad reflections centered at 0.34 and 0.22 nm which is typical of natural allophane as well as X-ray amorphous aluminosilicates [18–20].

Figure 2 exhibits the FT-IR spectrum of synthetic ALL and the characteristic absorption bands based on aluminosilicate can be clearly observed. The

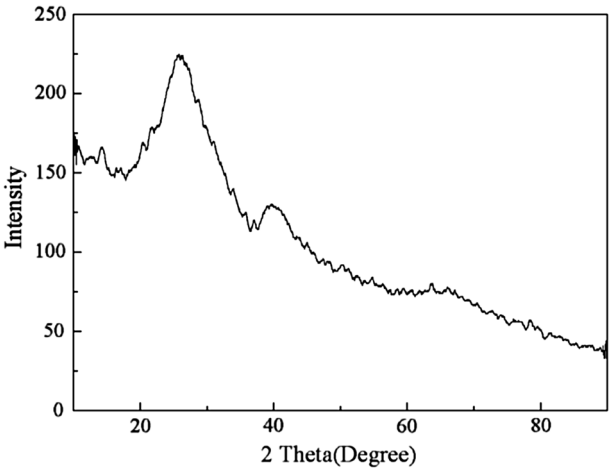

Fig. 1 XRD pattern of allophane

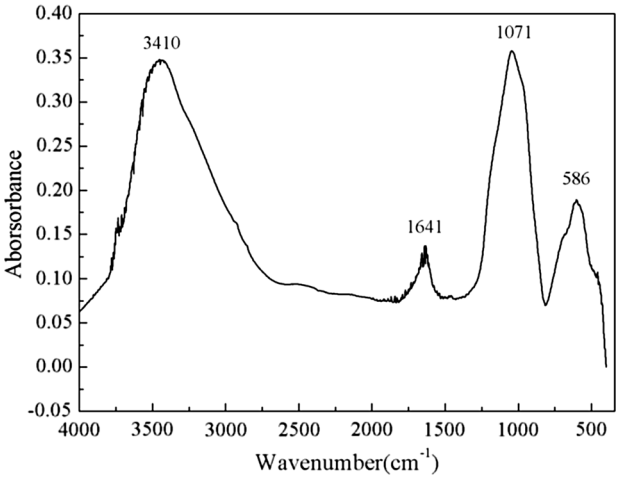

Fig. 2 FT-IR spectrum of the synthetic allophane

characteristic absorption centered at 3410 cm^{-1} is assigned to structural O–H, the absorption peak at 1071 cm^{-1} corresponds to Al–O or Si–O stretching, and those at 800–400 cm^{-1} is assigned to Si–O–X (X: Si or Al) stretching. An absorption band appeared at 1641 cm^{-1} is resulted from the O–H bending vibration of adsorbed water [17].

TG and DTG curves of ALL are shown in Fig. 3. The sharp weight loss between 25 and 100 °C is due to dehydration, while the gradual decrease in weight between 100 to 700 °C is attributed to the structural dehydroxylation [21]. Up to 700 °C, the total weight loss of ALL is about 28 %.

The XRD pattern (Fig. 1), FT-IR spectrum (Fig. 2), TG and DTG curves (Fig. 3) of ALL are in agreement with the results reported earlier [17–21]. The results above confirm that we have synthesized ALL successfully.

Limiting oxygen index (LOI) and UL-94 rating

Limiting oxygen index test is conducted and the related data are given in Table 1. From the LOI data, it can be seen that pure PP is a flammable polymer, and its LOI value is only 18. With total loading of 25 wt% IFR in PP, LOI value goes up to 27. When ALL was also added, the LOI value increases further. Initially, the LOI values of the PP/IFR blends enhance to 29 with 1 wt% addition of ALL. Subsequently, the LOI values of the PP/IFR composites increase from 29 to 35 when the addition of ALL reaches 2 wt%. However, the LOI value declines when the amounts of ALL increase. UL-94 results of the PP composites are also given in Table 1. The pure PP burns too fast and has no UL-94 level. In the case of PP/IFR, PP/IFR/ALL1, PP/IFR/ALL3, PP/IFR/ALL4 and PP/IFR/ALL5, only V-1 rating can be achieved. However, the PP/IFR/ALL2 samples can pass the V-0 rating. The LOI and UL-94 tests indicate that 2 wt% is the optimal addition of ALL for the PP/IFR systems to achieve the maximum flame-retardant property.

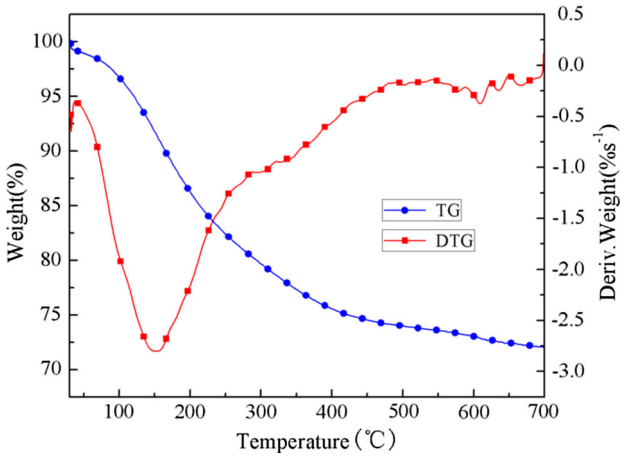

Fig. 3 TG and DTG curves of ALL

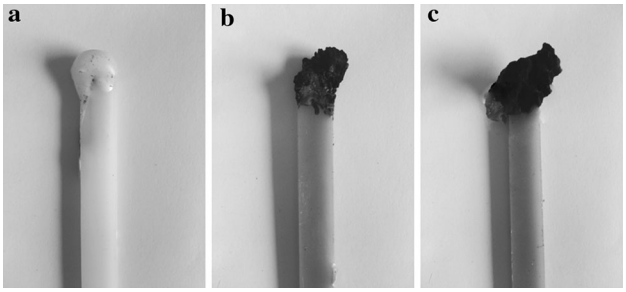

Fig. 4 Digital photographs of the specimens after LOI test **a** PP, **b** PP/IFR, **c** PP/IFR/ALL2

The LOI and UL-94 test results all illustrate that a proper amount of ALL could cause the best synergistic flame-retardant effect in the PP/IFR composites, which may be explained by that the dehydrogenation and the formation of char layer could be promoted by a small amount of ALL. When the amount of ALL is excessive, agglomeration will be caused and the homogeneity and carbonization function of the PP/IFR systems may be restrained which will lead to the decrease of LOI value and UL-94 level [22].

The digital photographs of the samples after LOI test are recorded in Fig. 4. It is clear that pure PP melts and drips heavily. With the addition of 25 wt% IFR, the melt dripping resistance of PP improves slightly. When 2 wt% ALL was also added, no dripping could be observed and an intumescent char layer was formed.

Cone calorimeter study

Cone calorimeter is generally used to estimate the flame retardancy of flame-retardant materials. Many important parameters can be obtained from cone

calorimeter such as the time to ignition (TTI), the heat release rate (HRR) especially the peak heat release rate (PHRR), the total heat release (THR), mass loss and the amount of smoke evolved, of which the most important is HRR and PHRR. Figures 5, 6, 7, 8 and 9 present the plots of PP flame-retardant composites. Table 2 lists the data in detail.

Figure 5 shows that neat PP burns rapidly after ignition and just one sharp HRR peak appears at 590 kW/m^2. The IFR containing PP composites show much lower HRR peaks at 179 kW/m^2. While the addition of 2 wt% ALL further enhances the flame retardancy of PP/IFR through an additional drop in the PHRR, the value of which is 138 kW/m^2. Furthermore, it is worth noting that two peaks of heat release rate (PHRR1 and PHRR2) appear in PP/IFR composite, which is a typical behavior of these types of systems [23]. PHRR1 is resulted from the formation of carbonaceous char. Fine cracks gradually produce on the surface of the protective char and result in the collapse of char structure, then creates PHRR2 [23, 24]. However, the heat release behavior of PP/IFR/ALL2 system is different from traditional PP/IFR system. After the PHRR, a large heat release plateau could be observed in PP/IFR/ALL2 and then it rapidly decreases. These results suggest that the synergistic effect between ALL and IFR may lead to the formation of high-quality char layer during combustion. This char protects the matrix from heat penetrating effectively and further combustion process is restricted. As a result, the heat evolved in tests reduces drastically.

Figure 6 shows the total heat release (THR) which is widely used to evaluate the fire safety of the materials. It can be seen that the THR significantly decreases when 25 wt% IFR is incorporated in PP. In the case of PP/IFR/ALL2, a further decrease of THR value can be observed. As shown in Fig. 7 and Table 2, PP/IFR/ALL2 system presents a much lower mass loss (ML) and the biggest residual mass is left at the end of burning. The stable char layer lowers the oxygen ingress, and thus prevents the further degradation of matrix. As a result, THR of PP/IFR/ALL2 decreases obviously.

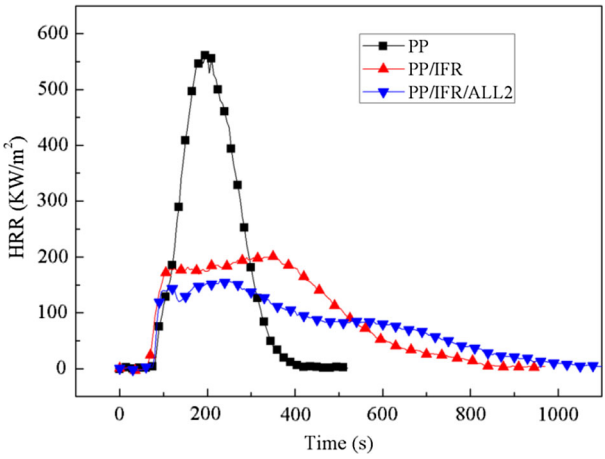

Fig. 5 HRR curves of selected composites

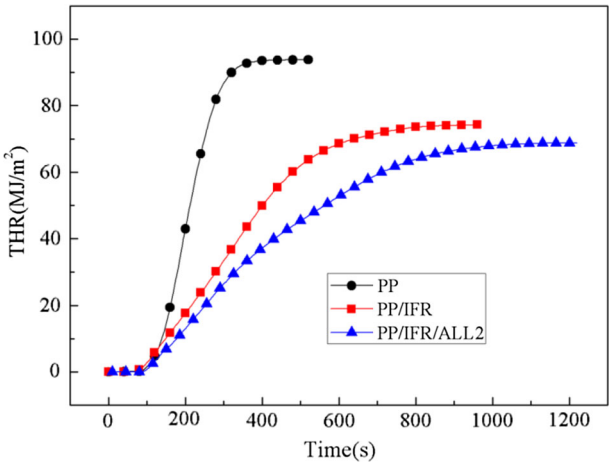

Fig. 6 THR curves of selected composites

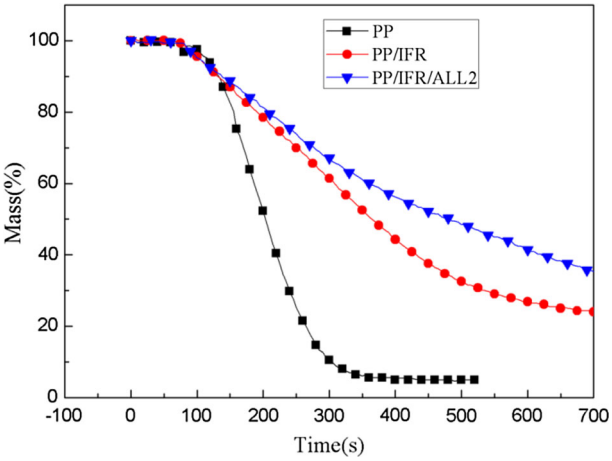

Fig. 7 Mass loss curves of selected composites

With regard to time to ignition (TTI), it starts earlier for all the composites (at 55 and 53 s) in comparison with neat PP (at 76 s) which is common in intumescent flame-retardant systems [25]. The FPI is listed in Table 2 to estimate the fire hazard more clearly, which is defined as the proportion of TTI to PHRR. FPI relates to the time available for escape in a full-scale fire situation. It is reported that there is a certain correlation between FPI of material and the time to flashover [26]. While the value of FPI reduces, the time to flashover increases and consequently fire hazard decreases. In comparison with neat PP (0.13) and PP/IFR (0.31) system, the PP/IFR/ALL2 system has the greatest value (0.38), which shows a step in the right direction in terms of fire hazard.

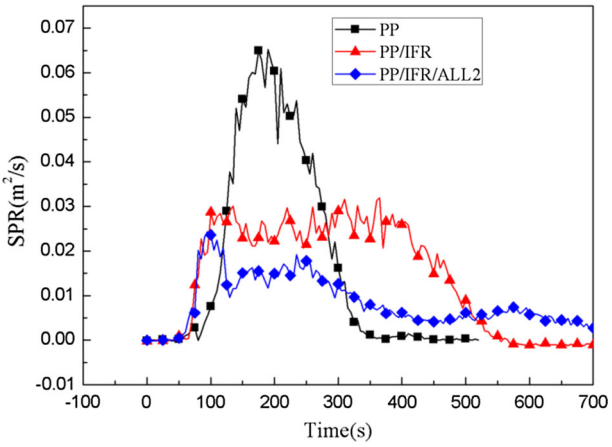

Fig. 8 SPR curves of selected composites

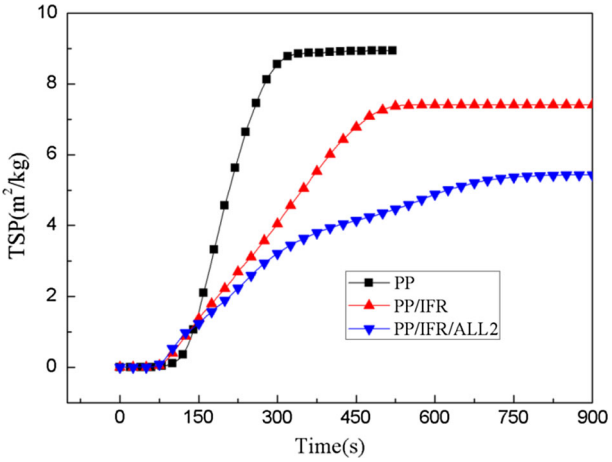

Fig. 9 TSP curves of selected composites

The emission of smoke is considered as another important parameter for the flame-retardant materials. The smoke production rate (SPR) and the total smoke production (TSP) curves of selected samples are presented in Figs. 8 and 9. In consistent with the HRR and THR curves, the addition of ALL in PP/IFR system could reduce SPR and TSP remarkably compared with neat PP and PP/IFR. The PSPR of PP/IFR/ALL2 is 0.02 m^2/s, while the PSPR of PP/IFR and neat PP is 0.04 and 0.07 m^2/s, respectively. The TSP of PP/IFR/ALL2 is also lower than PP/IFR and pure PP. The results above demonstrate that ALL combined with IFR performs better flame retardancy and smoke suppression when applied in PP.

Table 2 Cone calorimetry data of selected composites

Samples	TTI (s)	PHRR1 (kW/m^2)	PHRR2 (kW/m^2)	THR (MJ/m^2)	PSPR (m^2/s)	TSP (m^2/kg)	Char residue at 500 s/%	FPI
Pure PP	76	590	–	93	0.07	9.01	4.91	0.13
PP/IFR	55	179	200	74	0.04	7.48	32.68	0.31
PP/IFR/ ALL2	53	138	149	68	0.02	5.41	48.57	0.38

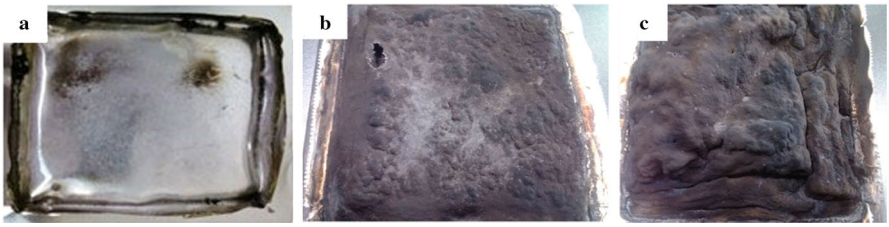

Fig. 10 Digital photographs of the residues after CONE test: **a** Pure PP; **b** PP/IFR; **c** PP/IFR/ALL2

It is well known that IFR system usually experiences an intense expansion and protective charred layers' formation [27]. Figure 10 displays the digital photographs of the residue chars for PP, PP/IFR and PP/IFR/ALL2 after cone calorimeter tests. Apparently, pure PP leaves no residue char after burning but PP/IFR composite gives an intumescent char layer. However, an expanded carbonaceous structure is formed with the addition of ALL, which can prevent the heat and mass transfer between the flame and the polymer substrate. Therefore, the further burning of the underlying materials is prevented and the HRR of PP reduces. These results further confirm the synergistic effect between ALL and IFR on enhancing the char formation and anti-dripping abilities for PP composites.

Comprehensively, all the data and curves above indicate that the presence of ALL in PP/IFR system showed synergistic effect on the flame-retardant properties of PP/IFR system, which was mainly due to the formation of the compact and continuous char layer on the surface of the materials during combustion processes.

Thermal stability

To investigate the synergistic effect of ALL in PP/IFR composites, the thermal decomposition behavior of the composites was investigated by TGA. Figure 11 shows the TG curves of pure PP and PP flame-retardant composites. The data obtained from the curves are summarized in Table 3.

It is found that only one-step weight loss about 99 wt% occurs in the range of 330–430 °C for pure PP, and the maximum mass loss rate appears at about 439 °C. Unlike PP, PP/IFR composite shows a lower T_{onset} at 242 °C and a higher T_{max} at 446 °C with a char residue of 11.25 wt% at 700 °C. The reason for the decrease of

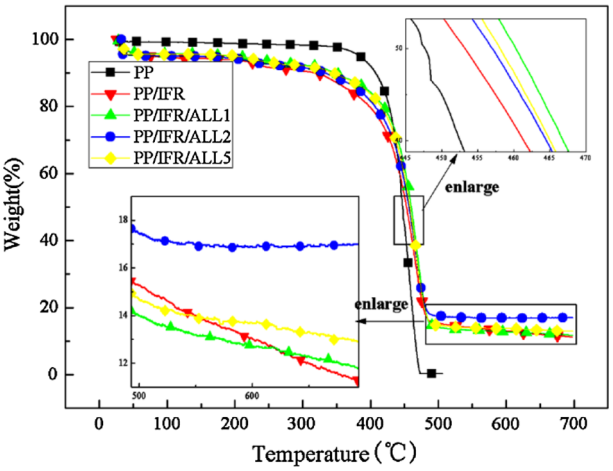

Fig. 11 TG curves of PP flame-retardant composites

Table 3 TGA data of PP composites

Sample	T_{onset} (°C)	T_{max} (°C)	Char residue at 700 °C (wt%)	
			Exp	Cal
PP	384	439	0.90	
PP/IFR	242	441	11.25	9.91
PP/IFR/ALL1	232	464	11.72	10.62
PP/IFR/ALL2	237	471	17.99	11.38
PP/IFR/ALL5	298	467	12.95	12.54

T_{onset} is that the decomposition of IFR in PP occurs at a relatively low temperature [28], which rapidly forms a protected char layer that prevents the inner matter from further decomposition. The increased T_{max} value indicates a delay in the maximum decomposition rate, which is consistent with intumescent function of this system. Compared with PP/IFR composite, PP/IFR/ALL2 system shows a lower T_{onset} at 237 °C. While the T_{max} of PP/IFR/ALL2 is 471 °C which is 30 °C higher than PP/IFR. And the char residue of PP/IFR/ALL2 composite was 17.99 wt% at 700 °C, as a contrast of 11.25 wt% for PP/IFR system. It is possible that the presence of ALL can promote char formation in the PP/IFR composites and form a char layer of better quality which can endure higher temperature and protect PP from decomposing. So the flame-retardant property is improved with the addition of ALL. The amount of theoretical residue left after heating can be calculated by linear combinations of the experimental char residue of each single component shown in TG curves. The theoretical char residues and experiment char yield at 700 °C are shown in Table 3. It can be seen that PP/IFR/ALL2 system shows a higher value in experimental char amount compared to the calculated char amount. The result indicates that a synergistic effect exists between IFR and ALL which can decrease the mass loss and improve the stabilization of the char layer at high temperature.

Morphologies and chemical compositions of the char residue

To analyze the chemical structure of the condensed phase, FT-IR spectra of carbonaceous residue after the CONE test of PP/IFR and PP/IFR/ALL2 system are shown in Fig. 12. The peak around 1000 cm^{-1} is attributed to the stretching vibration of P-O group which demonstrates an esterification occurring between APP and PER [29]. The absorbance at 1578 cm^{-1} is ascribed to the vibration of C=C in aromatized chars [25]. It is the result of carbonization reaction and the fracture of phosphate bonds. For PP/IFR/ALL2 composite, a band appears at 1100 cm^{-1} which is corresponding to silicoaluminophosphate (SAPO) [29]; however, this peak disappears in the case of PP/IFR composite. This suggests the silicoaluminophosphate (SAPO) structure formed during the combustion when ALL is added. SAPO is formed by the reaction of ALL and phosphoric acid. And the phosphoric acid is generated by the decomposition of IFR on heating. SAPO is a promising solid acidic catalyst and enhances the acid source (phosphoric acid) which takes part in the dehydration of the carbonific compounds to yield carbon char [13]. Because of the catalysis and enhancement of SAPO, phosphoric acid may further favor the oxidative dehydrogenation crosslinking charring process and increase the char yield. This leads to an enhancement in flame retardancy.

To analyze and reflect the effect of ALL in enhancing the fire resistance of PP composites, the char residue of PP/IFR and PP/IFR/ALL2 after cone calorimeter test was characterized by Raman spectra (Fig. 13). Raman spectra can evaluate the graphitization degree of carbon materials in terms of two characteristic bands: D band (1380 cm^{-1}, representing the unorganized carbon structure) and G band (1600 cm^{-1}, showing the graphitic structure) [30, 31]. The graphitization degree of char is a very important structural parameter. A higher graphitization degree of char means there is more perfect graphitic structure in the char residue. As we know that the char with lower graphitization degree has higher reactivity to oxidation, it will

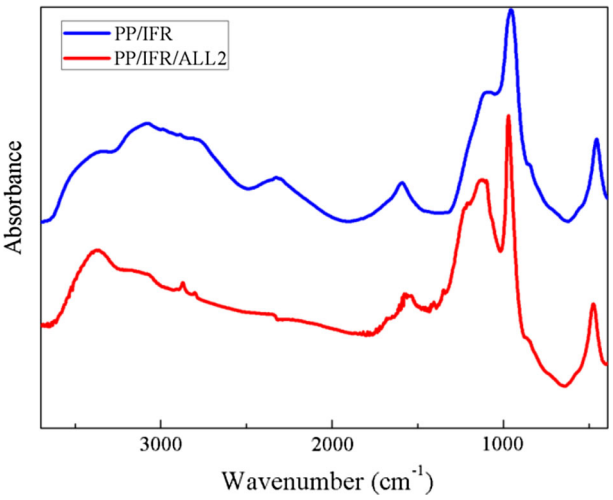

Fig. 12 FTIR spectra of residues after cone calorimeter test

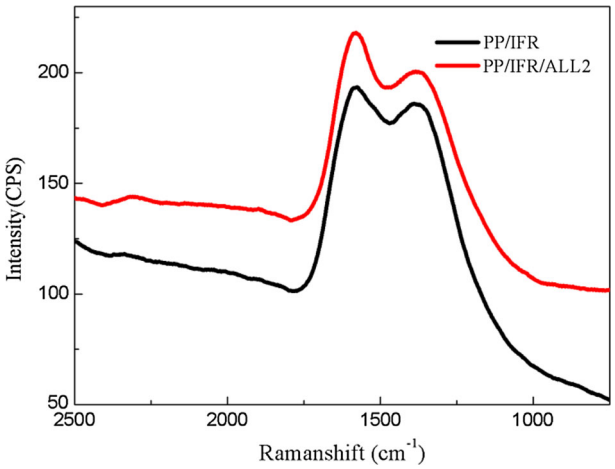

Fig. 13 Raman spectra of the residues for PP/IFR and PP/IFR/ALL2

turn out in the long time exposure to a high extent of heat flux as occurring in the cone calorimeter. However, a char in higher graphitization degree tends to give better protection of materials from thermal oxidation [31, 32]. The ratio of the integral peak intensity of the D band and G band, $R = I_D/I_G$, represents the graphitization degree of the chars [33]. From Fig. 13, the R value of PP/IFR/ALL2 was 1.1, while in the case of PP/IFR, it was 1.02 which indicates more graphitic structure formed in the char residue of PP/IFR/ALL2. This result further indicated that ALL combined with IFR could promote the formation of high graphitization degree char layer, therefore protect the matrix effectively.

To further investigate the synergistic effects of ALL on the charring of PP composites, the morphologies of char residues of PP/IFR and PP/IFR/ALL2 collected after cone calorimeter test were characterized by SEM, and the results are provided in Fig. 14. As shown in Fig. 14, although a relatively compact char layer was obtained in burning for PP/IFR, weak points of bubbles and cracks can be observed which is due to insufficient char formation during combustion. While the microstructure of char residue for PP/IFR/ALL2 displayed more homogenous and compact char layer when the char layer was observed under magnification of 5000 X. Based on the above analysis, we can conclude that the incorporation of ALL can generate more compact and intact char layer in the intumescent flame-retarded system so as to achieve a higher degree of fire retardation.

Mechanical properties

The mechanical properties of flame-retardant PP composites are also very important to be taken into consideration. Table 4 presents the tensile strength and impact strength of the flame-retardant PP composites. As expected, the tensile strength of PP/IFR decreases compared with pure PP, but increases when ALL is added. The composites containing 2 wt% ALL display the best tensile strength, when the content of ALL is more than 2 wt%, the tensile strength of the composites begins to decrease. In our work, it can be seen that no

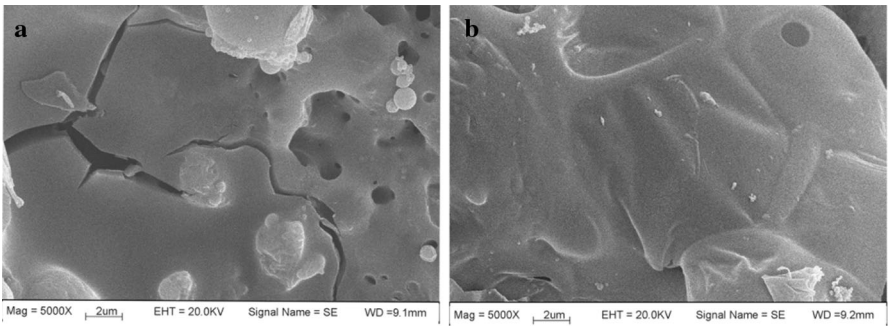

Fig. 14 SEM micrograph of residue char: **a** PP/IFR; **b** PP/IFR/ALL2

Table 4 Effect of ALL on tensile strength and impact strength of PP composites

Sample	Tensile strength (MPa)	Impact strength (kJ/m^2)
PP	22.81 ± 0.5	23.81 ± 0.8
PP/IFR	17.52 ± 0.3	8.62 ± 0.5
PP/IFR/ALL1	20.91 ± 0.4	9.48 ± 0.3
PP/IFR/ALL2	23.29 ± 0.3	10.79 ± 0.2
PP/IFR/ALL5	22.18 ± 0.5	9.11 ± 0.3

matter PP/IFR or PP/IFR/ALL composites, the impact strength all decreases compared to neat PP. However, the impact strength of PP/IFR is improved by the addition of ALL. It is worth noting that the addition of ALL not only can improve the flame retardancy but also can improve the tensile strength and impact strength of PP/IFR.

Conclusion

There was a noticeable synergism between ALL and IFR on the flame retardancy of PP. LOI value reached 35 and UL-94 V-0 rating was obtained in case of IFR (25 %) plus 2 % ALL. Indeed, ALL and IFR were able to cooperate in the char formation, as shown by flammability, cone calorimetry tests and thermogravimetry. CONE experiment confirmed that the addition of 2 wt% ALL markedly decreased the PHRR, HRR and THR of the compounds and combustion times were prolonged. TGA data showed the addition of ALL to the PP/IFR blends can improve their thermal stability, especially at a high temperature range above 500 °C and apparently promote char formation. FT-IR and SEM results showed that a SAPO structure containing compact and dense char layer was formed, which hindered the transfer of heat flow and combustible gases in the condensed phase. The mechanical properties of PP/IFR were improved by the loading of ALL.

Acknowledgments The authors gratefully acknowledge the financial supports of Jiangsu Overseas Research & Training Program for University Prominent Young & Middle-aged Teachers and Presidents, 2010 Enterprise Doctor Cluster Plan of Jiangsu Province and the Priority Academic Program Development of Jiangsu Higher Education Institutions (PAPD).

References

1. Hamzah MS, Hidayah IN, Mariatti M et al (2014) Dielectric and thermal properties of flame retardant fillers in polypropylene/ethylene propylene diene monomer composites. J Reinf Plast Compos 33:1931–1940
2. Shen H, Wang YH, Mai KC (2011) Effect of compatibilizers on thermal stability and mechanical properties of magnesium hydroxide filled polypropylene composites. Thermochim Acta 483:36–40
3. Wit CA (2002) An overview of brominated flame retardants in the environment. Chemosphere 46:583–624
4. Song P, Fang ZP, Tong LF et al (2008) Effects of metal chelates on a novel oligomeric intumescent flame retardant system for polypropylene. J Anal Appl Pyrolysis 82:286–291
5. Szustakiewicz K, Cichy B, Gazińska M et al (2013) Comparative study on flame, thermal, and mechanical properties of HDPE/clay nanocomposites with MPP or APP. J Reinf Plast Compos 14:1005–1017
6. Wang XL, Song Y, Bao JC (2008) Synergistic effects of nano-$Mn_{0.4}Zn_{0.6}Fe_2O_4$ on intumescent flame-retarded polypropylene. J Vinyl Addit Technol 14:120–125
7. Yuan WH, Chen HR, Chang RR et al (2011) Synthesis and characterization of NaA zeolite particle as intumescent flame retardant in chloroprene rubber system. Particuology 9:248–252
8. Sun LS, Qu YT, Li SH (2012) Co-microencapsulate of ammonium polyphosphate and pentaerythritol and kinetics of its thermal degradation. Polym Degrad Stab 97:404–409
9. Chiu SH, Wang WK (2012) Dynamic flame retardancy of polypropylene filled with ammonium polyphosphate, pentaerythritol and melamine additives. Polymer 39:1951–1955
10. Chen XL, Jiao CM (2009) Synergistic effects of hydroxy silicone oil on intumescent flame retardant polypropylene system. Fire Saf J 44:1010–1014
11. Bai G, Guo CG, Li LL (2014) Synergistic effect of intumescent flame retardant and expandable graphite on mechanical and flame-retardant properties of wood flour-polypropylene composites. Constr Build Mater 50:148–153
12. Ozkaraca AC, Kaynak C (2012) Contribution of nanoclays to the performance of traditional flame retardants in ABS. Polym Compos 33:420–429
13. Attia NF, Hassan MA, Nour MA et al (2013) Flame-retardant materials: synergistic effect of halloysite nanotubes on the flammability properties of acrylonitrile–butadiene–styrene composites. Polym Int 63:1168–1173
14. Chen YJ, Fang ZP, Yang CZ et al (2010) Effect of clay dispersion on the synergism between clay and intumescent flame retardants in polystyrene. J Appl Polym Sci 115:777–783
15. Iyoda F, Hayashi S, Arakawa S et al (2012) Synthesis and adsorption characteristics of hollow spherical allophane nano-particles. Appl Clay Sci 56:77–83
16. Abidin Z, Matsue N, Henmi T (2007) Differential formation of allophane and imogolite: experimental and molecular orbital study. J Comput Aided Mater Des 14:5–18
17. Ohashi F, Wada SI, Suzuki M et al (2002) Synthetic allophane from high-concentration solutions: nanoengineering of the porous solid. Clay Miner 37:451–456
18. Brigatti MF, Galan E, Theng BKG (2006) Structures and mineralogy of clay minerals. Handb Clay Sci 1:19–69
19. Parfitt RL (2009) Allophane and imogolite: role in soil biogeochemical processes. Clay Miner 44:135–155
20. Okada K, Nishimuta K, Kameshima Y et al (2005) Effect on uptake of heavy metal ions by phosphate grafting of allophane. J Colloid Interface Sci 286:447–454
21. Krrlclwe Y (1974) Dehydration of allophane and lts structural formula. Am Mineral 59:1094–1098
22. Lewin M (2001) Synergism and catalysis in flame retardancy of polymers. Polym Adv Technol 12:215–222
23. Bourbigot S, Bras ML, Duquesne S et al (2004) Recent advances for intumescent polymers. Macromol Mater Eng 289:499–511
24. Duquesne S, Samyn F, Bourbigot S et al (2008) Influence of talc on the fire retardant properties of highly filled intumescent polypropylene composites. Polym Adv Technol 19:620–627
25. Su XQ, Yi YW, Tao J et al (2014) Synergistic effect between a novel triazine charring agent and ammonium polyphosphate on flame retardancy and thermal behavior of polypropylene. Polym Degrad Stab 105:12–20

26. Wang BB, Tang QB, Hong NN et al (2011) Effect of cellulose acetate butyrate microencapsulated ammonium polyphosphate on the flame retardancy, mechanical, electrical, and thermal properties of intumescent flame-retardant ethylene–vinyl acetate copolymer/microencapsulated ammonium polyphosphate/polyamide-6 blends. ACS Appl Mater Interface 3:3754–3761
27. Ribeiro SP, Estevão LR, Pereira CMC et al (2013) Mechanism of action of different d-spacings clays on the intumescent fire retardance of polymers. J Appl Polym Sci 130:1759–1771
28. Wang DY, Liu Y, Wang YZ et al (2007) Fire retardancy of a reactively extruded intumescent flame retardant polyethylene system enhanced by metal chelates. Polym Degrad Stab 92:1592–1598
29. Ma HY, Tong LF, Xu ZB et al (2008) Intumescent flame retardant-montmorillonite synergism in ABS nanocomposites. Appl Clay Sci 42:238–245
30. Ma HY, Fang ZP (2012) Synthesis and carbonization chemistry of a phosphorous–nitrogen based intumescent flame retardant. Thermochim Acta 543:130–136
31. Ma HY, Tong LF, Xu ZB et al (2007) Synergistic effect of carbon nanotube and clay for improving the flame retardancy of ABS resin. Nanotechnology 18:1–8
32. Tai QL, Yuen RKK, Yang W et al (2012) Iron-montmorillonite and zinc borate as synergistic agents in flame-retardant glass fiber reinforced polyamide 6 composites in combination with melamine polyphosphate. Compos Part A Appl Sci Manuf 43:415–422
33. Huang NH, Chen ZJ, Wang JQ et al (2010) Synergistic effects of sepiolite on intumescent flame retardant polypropylene. Express Polym Lett 4:743–752